# Improved Projectile Boattail

Anders S. Platou*
*U.S. Army Ballistic Research Laboratories, Aberdeen Proving Ground, Md.*

**A series of projectile boattails has shown improved aerodynamic performance over the standard conical boattail. These boattails have equal or lower drag and an improved gyroscopic stability. Their Magnus and damping characteristics appear to be satisfactory so that the projectile should be dynamically stable. Also, these boattails increase the projectile wheel base considerably, thereby decreasing the balloting in the gun tube. The improved aerodynamic performance could lead to longer ranges, larger payloads, or lower spin rates for furture projectiles.**

## Nomenclature

$C_D$ = drag/$\frac{1}{2}\rho V^2 S$, positive direction is aft
$C_{D_0}$ = zero angle of attack drag coefficient
$C_{D_{\alpha^2}}$ = drag coefficient slope due to angle of attack (from $C_D = C_{D_0} + C_{D_{\alpha^2}}\alpha^2$)
$C_{\ell_p}$ = roll damping moment coefficient—negative moment tends to decrease spin
$C_{\ell_\delta}$ = roll moment coefficient due to fin cant —positive moment tends to increase spin
$C_m$ = pitching moment/$\frac{1}{2}\rho V^2 Sd$, moment center is 0.6 $\ell$ calibers from nose (1 caliber = 4.25 or 2.25 in.). Positive moment is due to positive normal force ahead of the moment center
$C_{m_\alpha}$ = $dC_m/d\alpha$ at $\alpha = 0°$ per rad
$C_{m_p}$ = Magnus moment/$\frac{1}{2}\rho V^2 Sd(pd/V)$, moment center is 0.6 $\ell$ calibers from nose. Positive moment is due to positive Magnus force ahead of moment center
$C_{m_{p_\alpha}}$ = $dC_{m_p}/d\alpha$ at $\alpha = 0°$ per rad
$C_{m_q} + C_{m_{\dot\alpha}}$ = damping moment/$\frac{1}{2}\rho V^2 Sd(q_t d/V)$
$C_N$ = normal force/$\frac{1}{2}\rho V^2 S$, positive direction is up
$C_{N_\alpha}$ = $dC_N/d\alpha$ at $\alpha = 0°$ per rad
$C_{N_p}$ = Magnus force/$\frac{1}{2}\rho V^2 S(pd/V)$, positive direction is to right, looking upstream
$C_{N_{p_\alpha}}$ = $dC_{N_p}/d\alpha$ at $\alpha = 0°$ per rad
$C_{n_0}$ = Magnus or side moment at zero spin
$C_{Y_0}$ = Magnus or side force at zero spin
$d$ = body diameter and reference length
$I_x$ = axial moment of inertia
$I_y$ = transverse moment of inertia
$k_x$ = axial radius of gyration
$k_y$ = transverse radius of gyration
$M_{CP}$ = Magnus force center of pressure
$N_{CP}$ = normal force center of pressure
$p$ = body axial spin rate (positive is clockwise looking upstream), rad/sec
$q_t$ = complex transverse angular velocity
$S$ = body area = $\pi d^2/4$
$S_d$ = dynamic stability = $\dfrac{2(C_{L_\alpha} + k_x^{-2} C_{m_{p_\alpha}})}{C_{L_\alpha} - C_D - k_y^{-2}(C_{m_q} + C_{m_{\dot\alpha}})}$
$S_g$ = gyroscopic stability = $\dfrac{[(I_x/I_y)\,(pd/V)]^2}{(2\rho Sd^3/I_y)C_{m_\alpha}}$
$V$ = freestream velocity
$\alpha$ = angle of attack
$\delta$ = cant angle of fin or twisted surface
$\rho$ = freestream air density
$\delta_F C_{\ell_\delta} + (pd/V)C_{\ell_p}$ = roll moment/$\frac{1}{2}\rho V^2 Sd$

Presented as Paper 74-779 at the AIAA Mechanics and Control of Flight Conference, Anaheim, California, August 5-9, 1974; submitted September 16, 1974; revision received June 30, 1975. A previously published article had the same title. See Ref.1.

Index categories: LV/M Aerodynamics; LV/M Configurational Design; LV/M Dynamics, Uncontrolled.

*Aerospace Engineer. Member AIAA.

## Introduction

THE main purpose of a projectile boattail is to reduce drag, over that of a cylindrical boattailed projectile† (Fig. 1), thereby increasing the range of the projectile. In past years various geometric shapes (a conical boattail has been the post popular) have been used to form the boattail and have depended on the reduced base area to reduce the drag. These boattails have worked well in reducing the drag; however, all of them develop a negative lift on the boattail, which increases the unstable pitching moment and reduces the gyroscopic stability. These boattails (especially the conical boattail) also generate large Magnus forces and moments at transonic velocities, which can adversely affect the dynamic stability of the projectile. Satisfactory gyroscopic and dynamic stability must be maintained so that the average angle of attack remains within low limits as the projectile moves along its trajectory.

Recently, the BRL has experimented with a series of boattail shapes, which do not have axial symmetry and which have a number of advantages over the axisymmetric boattails. These boattails are formed by cutting the main projectile cylinder with planes, inclined at a small angle to the main projectile axis, such that flat surfaces are created on the boattail. The flat surfaces increase the boattail lift so that the unstable pitching moment is decreased and the drag is reduced by the smaller base area. Also, these boattails have elements of the main cylinder extending to the base, which increases the

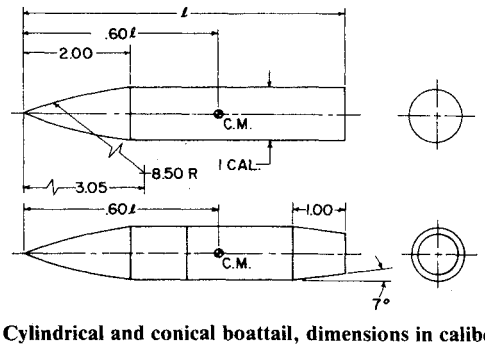


**Fig. 1 Cylindrical and conical boattail, dimensions in calibers ($\ell = 4, 5, 6, 7$).**

†Previously known as a square-base configuration, but changed here to avoid confusion with the new version 1) boattail.

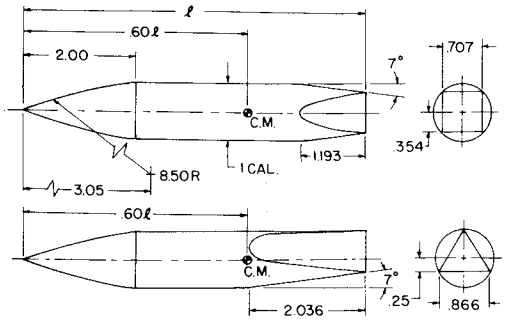


**Fig. 2 Square and triangular boattail, dimensions in calibers ($\ell = 5, 6, 7$).**

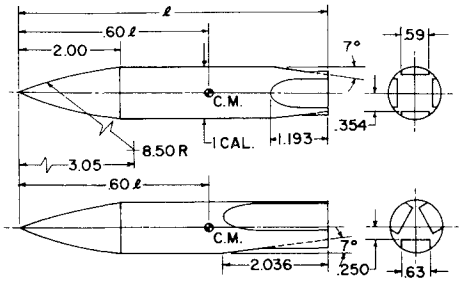


**Fig. 3 Added lifting surfaces, dimensions in calibers ($\ell = 5, 6, 7$).**

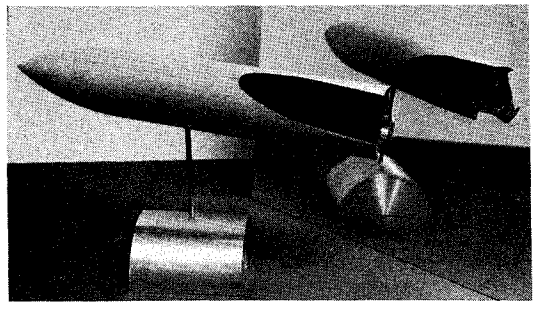

**Fig. 4 Canted boattail.**

wheel base over that of the axisymmetric boattails. The increased wheel base will reduce gun tube balloting and possibly reduce muzzle jump and gun tube wear. Possible versions of these boattails are:

1) A boattail formed using four cutting planes so that the base becomes an inscribed square (Fig. 2).[‡] 2) A boattail formed using three cutting planes so that the base becomes an inscribed triangle (Fig. 2).[‡]. 3) Boattails formed similar to 1) or 2) but with the cutting plane widths limited so that added lifting surfaces are formed at the base corners (Fig. 3).[‡] 4) Boattails formed similar to 1), 2), and 3) but with cutting planes canted so as to reduce the roll damping during flight (Fig. 4).[‡] 5) A boattail formed by eliminating all of the main body cylinder volume not included inside the volume of two orthogonal wedges (Fig. 5).[§] This version can be extended to zero base area or can be cut off at any station to form a cruciform base.

Characteristics of these new boattails which may be important are:

1) The flat surfaces generated on the boattails may act as lifting surfaces, thereby increasing the lift on the aft portion of the projectile and decreasing the unstable pitching moment. 2) All of these boattails have a better cross-sectional area distribution than the conical boattails (Fig. 6). This reduces the rapidity of flow expansion over the boattail and will reduce the viscous losses and maintain the Bernoulli head in

[‡] Patent No. 3,873,048.

[§] Patent disclosure has been submitted.

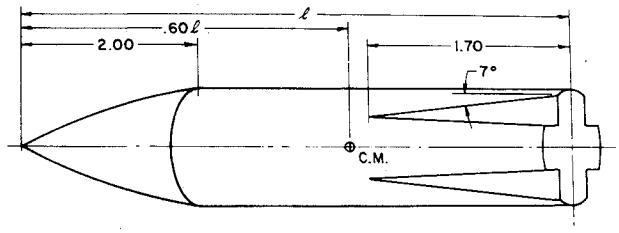


**Fig. 5 Wind-tunnel model of cruciform wedge boattail, dimensions in calibers ($\ell = 5, 6, 7$).**

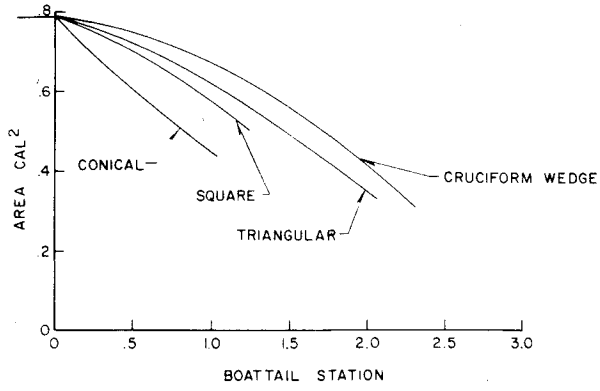


**Fig. 6 Cross-sectional areas of 7° boattails.**

the flow. 3) The cylinder elements which extend to the base will form crude rotating fins, which should have Magnus forces acting opposite to those on the body.[2] The opposing forces should minimize the resultant Magnus force and moment about the projectile center of gravity.

Aerodynamic tests on these boattail configurations have been made to verify these characteristics and also to find the configuration having the best overall aerodynamic performance. These tests have been run in U. S. Government wind tunnels and ranges which were available for these purposes.

## Test Facilities

The wind-tunnel facilities used for the tests were:

1) The NASA Ames Research Center 12-ft subsonic wind tunnel, $M = 0.5$, $0.7$, and $0.9$, 4¼-in. model, Re/ft = 1.35-2.8 × $10^6$ (Re/m = 4.23-9.2 × $10^6$). 2) The Naval Ship Research and Development Center (NSRDC) 7 × 10-ft transonic wind tunnel, $M = 0.5$, $0.7$, $0.9$, $0.04$, and $0.98$, 4¼-in. model, Re/ft = 2.65-4.0 × $10^6$ (Re/m = 8.68-13.1 × $10^6$). 3) The Ballistic Research Laboratories (BRL) 1-ft supersonic wind tunnel, $M = 1.75$-$4.0$, 2¼-in. model, Re/ft = 3.6-7.0 × $10^6$ (Re/m = 11.8-23.0 × $10^6$).

The range facility used for the tests is the Ballistic Research Laboratories (BRL) aerodynamic range, $M = 0.5$ to $4.0$, 20-mm models, atmospheric free-flight Reynolds numbers.

## Wind-Tunnel Models

These boattails were tested using the Army-Navy spinner rocket nose and body with the complete configurations of 5, 6, or 7 calibers in length. Two sizes of models, 2¼-in. (5.715-cm) and 4½-in. (10.795-cm) diameters, were required for the wind-tunnel tests because of the variation in the tunnel sizes available for the different speed ranges. The models were designed according to specifications already described.[3] They consist of a central body mounted on ball bearings and a strain-gage balance with various tails and noses attached to the central body. Variations in the lengths of the noses and tails made it possible to test body lengths of 5, 6, or 7 calibers. Tails for each boattail version (listed previously) were made

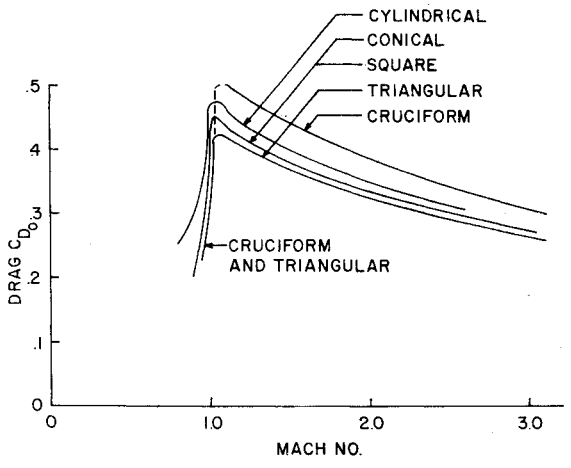


**Fig. 7 Zero yaw drag of improved boattails.**

by using a 7° cutting plane angle for both the 2¼-in. and 4¼-in. diameter models. Also, a straight cylindrical tail and a 1 caliber long 7° conical boattail were available for comparison (Fig. 1). Each boattail version could be tested on the 2¼-in. diameter body with configuration lengths of 5, 6, or 7 calibers; however, the 5-caliber, 4¼-in. model was limited to the straight cylinder, the conical boattail, and the square boattail. Six- and seven-caliber, 4¼-in. diameter models of all of the boattail versions have been tested.

## Range Models

Five-caliber long, 20-mm diameter models of these configurations have been fired in the BRL aerodynamic range at transonic and supersonic velocities. These models are solid aluminum and have their centers of gravity approximately 60% of the length from the nose. All of the pitching and Magnus moment data have been transferred to the 60% location. The models were launched from two rifled barrels having twists of one revolution in 15.2 calibers and 1 revolution in 19 calibers.

## Results and Analysis

The results presented in this paper complement, add to, and modify the results already presented[1] and present the main aerodynamic results now available on the new boattails. The results are based on the experimental free-flight range and wind-tunnel data obtained on the 5-caliber long models. Some data have been obtained on the 6- and 7-caliber wind-tunnel models, but these data are not sufficient to give a complete picture. The range flights yield the free-flight drag, pitch data, Magnus, roll damping, and pitch damping moments at low angles of attack. The wind-tunnel tests yield angle of attack drag,[4] detailed pitch data, Magnus force and moment over a range of spin and range of angle of attack (−10 to +15°). Most of the data are presented here as faired curves for clarity and brevity; however, the detailed data points are available at BRL to the interested reader.

All of the wind-tunnel data have been obtained using a boundary-layer transition strip located 1 caliber aft of the nose. The range models did not use a transition strip, but depended on firing conditions to trip the boundary layer. Therefore, as well as can be determined all of the data presented here are for the case of a turbulent boundary layer over the configuration. This is similar to projectile flights where the rough surface is sufficient to maintain a turbulent boundary layer. Previous tests on smooth wind-tunnel bodies without a transition strip have shown that the boundary-layer transition moves with spin. This, in some cases, results in nonlinear variations in the Magnus characteristics with spin.

[4] Some wind-tunnel drag data are available, but breakage of drag balances due to model spin resonance with the drag link has caused severe problems in obtaining drag data with the model spinning.

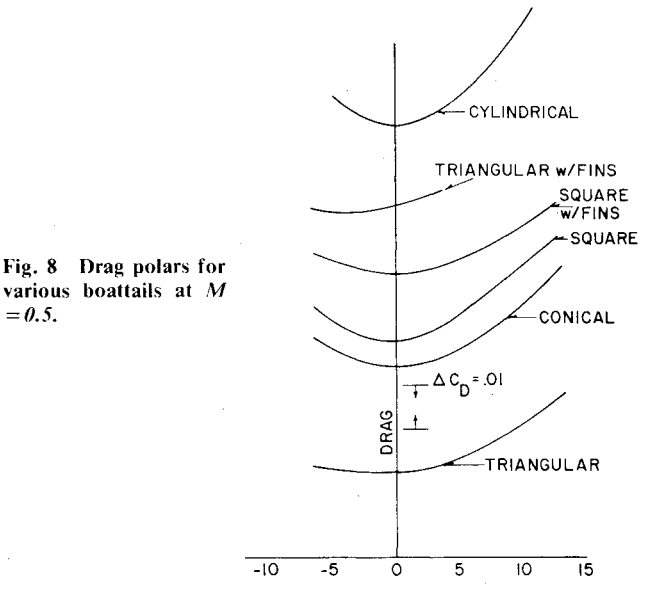


**Fig. 8 Drag polars for various boattails at $M = 0.5$.**

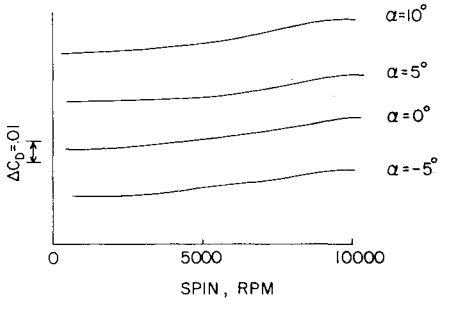


**Fig. 9 Drag variation due to spin on straight square boattail at $M = 0.9$.**

The zero angle of attack drag coefficient $C_{D_0}$ for the various boattails are compared in Fig. 7. The triangular boattail has the lowest drag while the square boattail has a drag near the conical boattail. The cruciform boattail has the highest drag of all the configurations at supersonic speeds, which is apparently due to low base pressures. The high drag rules out the use of the cruciform tail for long-range projectiles; however, its low drag at high subsonic speeds and its relatively high stability at all Mach numbers, as explained later, may make it useful for other purposes.

The low drag of the triangular base is due to two factors. First, the gradual flow expansion over the boattail maintains a more constant Bernoulli head, and second, the triangular boattail has a small base area. The more constant Bernoulli head deters separation and lowers the viscous drag, while the small base decreases the base drag.

The geometric asymmetry of the triangular boattail may also decrease the drag at low angles of attack. At zero spin the asymmetry produces an asymmetric drag polar (Fig. 8), so that drag values at constant angle of attack with spin will be the average drag between plus and minus angles of attack. It appears that this will increase $C_{D_{\alpha^2}}$ at least at low angles of attack; however, this thought has not been thoroughly investigated, due to strain-gage balance difficulties.

The first transonic wind-tunnel tests at Ames and NSRDC and a few free-flight tests at transonic velocities showed that the drag of the added lifting surface version (Fig. 3) is considerably higher than that of versions 1 or 2 (Fig. 2). At present the higher drag is attributed to the added base area and possibly a lower base pressure. This plus the minimal in-

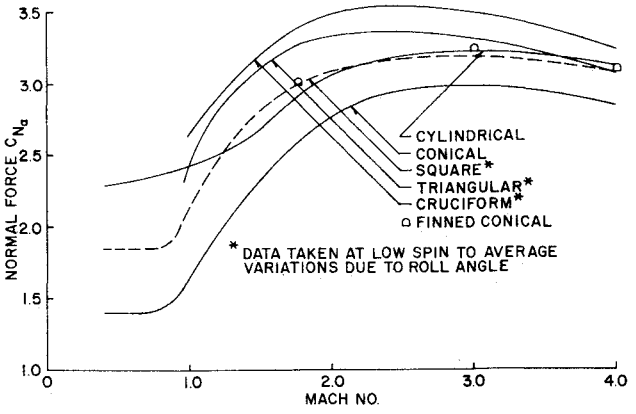


**Fig. 10 Normal force on improved boattail configurations.**

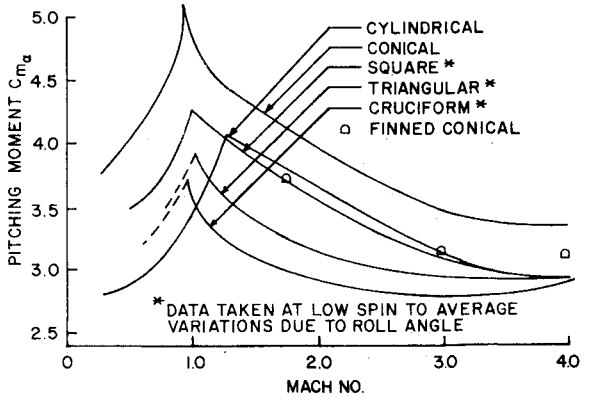


**Fig. 11 Pitching moments on improved boattails.**

crease in stability have curtailed further testing of version 3 to a later data.

The wind-tunnel tests have shown some variation of drag with spin on the new boattails (Fig. 9). The straight boattails have minimum drag at zero spin, while the twisted boattails have minimum drag at the twist rate. Again, the available data to confirm these results are limited, due to mechanical failure of the drag balance.

The gyroscopic stability of a projectile is directly proportional to the spin squared and inversely proportional to the aerodynamic pitching moment.** Since stable flight of a projectile requires that the gyroscopic stability remain above 1, it behooves the designer to select a projectile shape having the best pitching moment. Conical boattails reduce the normal force (Fig. 10) and increase the unstable pitching moment, especially at transonic velocities (Fig. 11). However, as seen in Figs. 10-12, the new boattails not only reduce the unstable pitching moments at all Mach numbers below that of the conical boattails, but at all supersonic Mach numbers of interest improve the pitching moment over that of the cylindrical tail. For the first time in artillery projectile design, a boattail which not only decreases drag but also increases the stability of the projectile can be employed. This could aid projectile design for, in most instances, the projectile design is governed by the maximum unstable pitching moment attained at any Mach number within the projectile flight envelope.

Some interest has been shown in comparing these boattails to a conical boattail with fins or strakes. However, a direct comparision is impossible with previous data since the finned boattails have not been tried on other projectile shapes. To obtain a direct comparison a 1-caliber long, 7° conical boattail with 4 in.-caliber fins was tested on the 2¼-in. wind-tunnel model at supersonic speeds. The results (Figs. 10 and

**All presented pitching moments are about a c.g. located 60% of the body length aft of the nose.

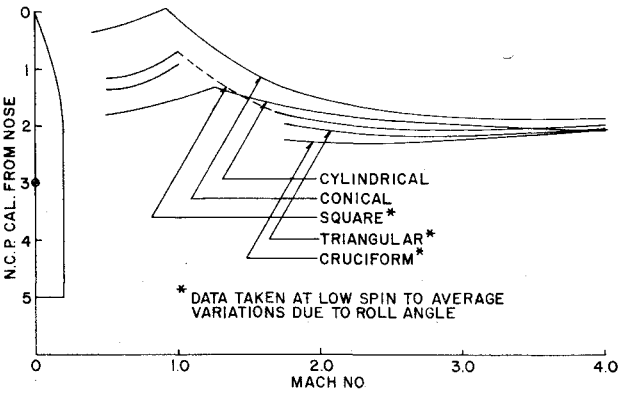


**Fig. 12 Normal force center of pressure on improved boattails.**

**Table 1 Range firings of boattails with 0 and 1/15 (rev/cal) twists**

| Type of boattail | $C_{l_p}$ | $C_{l_\delta}$ |
|---|---|---|
| Square | -0.055 | +0.037 |
| Triangular | -0.098 | +0.084 |
| Cruciform | -0.073 | +0.063 |
| Conical or cylindrical | -0.015 | 0 |

11) show that the finned conical boattail has about the same normal force and pitching moment as the square boattails, but will have higher drag than the square boattail since the square boattail drag is the same as the bare conical boattail. The finned boattail drag will be greater than the base conical boattail, due to the additional fin drag.

One of the aerodynamic problems of the new boattails is the high roll damping inherent in the straight configurations. Roll damping moment coefficients up to −0.1 were measured during the range flights which is sufficient to despin a typical projectile to instability during flight. To circumvent this, it is necessary to twist or cant the boattails so that spin will be maintained during the flight. Range firings of these boattails with 0 and 1/15 (rev/cal) twists yield the rolling moments given in Table 1.

Because the flow helix angle ($pd/V$) on a typical projectile increases during flight, the optimum twist for the boattail should be a value slightly lower than the gun twist. After launch of the projectile at the gun twist rate, the projectile would despin slightly, due to the lower boattail twist, thereby maintaining a more constant $pd/V$.

Even though it is not possible theoretically to predict the Magnus force on a projectile, it is possible by studying shadowgraphs and analyzing the force and moment test results to visualize the mechanisms producing the Magnus force. The picture which is visualized is that of an aerodynamic body composed of the actual projectile body surrounded by a warpable, viscous, aerodynamic body made up of the boundary layer.

At all Mach numbers the Magnus force is generated to a large extent by the shape of the boundary layer. and the shape in turn is influenced greatly by the viscous twist or warpage due to the projectile spin,[4] At zero angle of attack the warpage of the boundary layer due to spin is axisymmetric about the main centerline, so that the resulting aerodynamic forces and moments are zero except for drag and rolling moment. At small angles of attack, the boundary layer thickens on the lee side of the body, but at zero spin the boundary layer maintains mirror symmetry. A normal force and pitching moment are generated, but the side forces and moments remain zero. With spin the thickened portion of the boundary layer twists in the direction of spin, all symmetry is destroyed, and a side force and moment are generated.

If a conical boattail is used in place of the cylindrical tail, at subsonic or transonic velocities, the boundary layer thickens

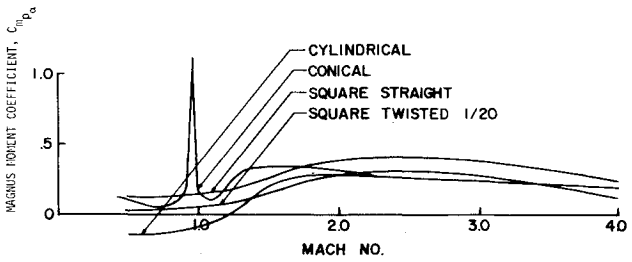


**Fig. 13 Magnus moments on improved boattails at low angles of attack.**

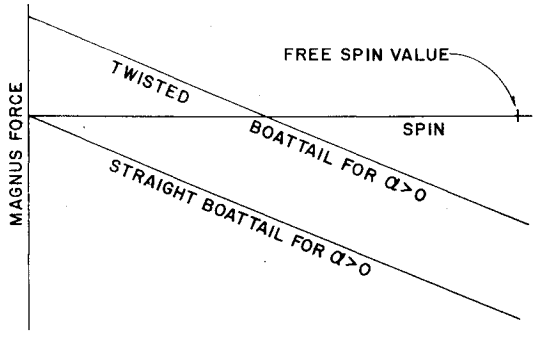


**Fig. 14 Side and Magnus forces on straight and twisted boattails.**

due to the flow expansion over the boattail. The thicker boundary layer is distorted more and a larger Magnus force is created (Fig. 13).[5] At supersonic speeds the Prandtl-Meyer expansion over the conical boattail holds the boundary layer to thinner values, so that large increases in Magnus force do not occur. The large increase in Magnus force and moment caused by the conical boattail at transonic velocities may be sufficient to destabilize an already marginally (gyroscopic) stable projectile[6] by causing large changes in dynamic stability.

Wind-tunnel and range tests on the new boattails indicate that no large Magnus forces and moments are generated at any of the tested Mach numbers (Fig. 13). The wind-tunnel tests at $M>1$ show the Magnus force and moments to be linear over the spin range tested (Fig. 14) and approximately linear over an angle-of-attack range of at least $\pm 3°$ (Fig. 15).[††] When nonlinearities do occur they appear to be in the direction of decreasing Magnus force and moment.

The side force generated on the twisted boattails modifies the above boundary-layer picture appreciably and results in small Magnus forces.[‡‡] At small angles of attack and zero spin the boundary layer is distorted by the twist in the opposite direction from the intended spin. For a right-hand twist the thick or lee side of the boundary layer twists to the left and creates a side force to the right. When the body spins in the direction intended or caused by the twist a Magnus force is generated to the left (Fig. 14).[§§] As the spin increases the combined side force is less than on a straight boattail configuration. From Fig. 14 it can be seen that, for a given $\alpha$, the side force and moment for a twisted boattail can be expressed as

$$C_Y = C_{Y_0} + C_{N_p} pd/V$$

$$C_n = C_{n_0} + C_{n_p} dp/V$$

[††] Additional subsonic and transonic wind tunnel tests must be run to verify this at the lower speed ranges. The subsonic and transonic wind-tunnel tests run to date have given sketchy Magnus results, due to the high sensitivity of Magnus characteristics to tunnel turbulence and flow inclination.

[‡‡] Fig. 16 of Ref. 1 is in error. At the time these data were taken, the offsets, (*a* and *b*) mentioned in this paragraph were not measured.

[§§] This was also noticed by Sylvester in Ref. 7.

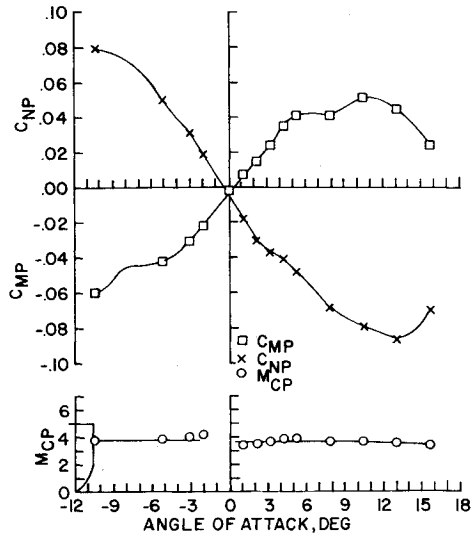


**Fig. 15 Magnus characteristics of triangular boattail at $M=2.5$, $pd/V=0.27$, $R_{dia}=0.94\times10^6$.**

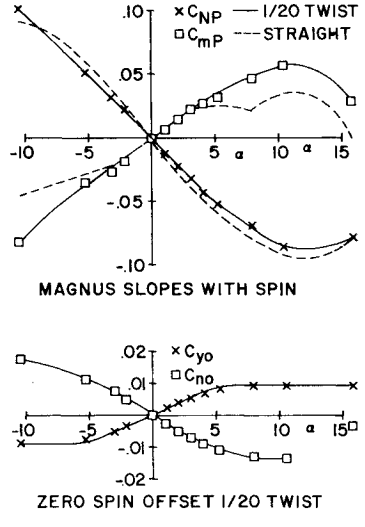


**Fig. 16 Magnus offsets and slopes on triangular boattail at $M=2.5$, $R_{dia}=950{,}000$.**

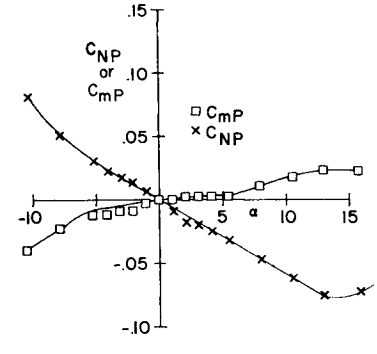


**Fig. 17 Magnus characteristics of triangular boattail with a 1/20 twist at a spin rate ($pd/V=0.412$), $M=2.5$, $R_{dia}=950{,}000$.**

where $C_{Y_0}$ and $C_{n_0}$ are the zero spin offsets at each angle of attack and $C_{N_p}$ and $C_{m_p}$ are the Magnus slopes at each angle of attack. These have been determined from wind-tunnel tests (Fig. 16) at supersonic speeds. It can also be seen that $C_{N_{p_\alpha}}$ and $C_{m_{p_\alpha}}$ are spin dependent (Fig. 17) for the twisted configurations and must be evaluated for all spin rates ($pd/V$) encountered during flight. References 8 and 9 present Magnus data on finned boattail configurations, and even though these data show fins reduce the Magnus properties, they do not indicate the zero spin offset shown by the BRL data.

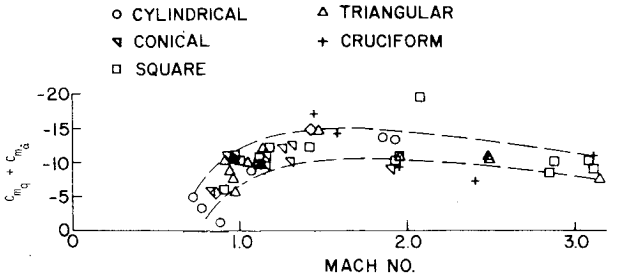


**Fig. 18 Damping in pitch of various boattails.**

Aerodynamic pitch damping measurements have been limited to range data and indicate that the aerodynamic damping is independent of the configuration (Fig. 18). This is surprising for the lifting surfaces on the new boattails should increase the pitch damping. No pitch damping data are available on a corresponding finned boattail configuration; however, unpublished data on the Navy 5-in./54 projectile with and without boattail fin show the same degree of damping. Possibly, the longer 6- or 7-caliber configuration will show a difference in the damping coefficient when they are tested.

## Conclusions

The aerodynamic data obtained show that all of the new boattails change the aerodynamic characteristics of projectile considerably: 1) The new boattails improve the pitching moment of projectiles over that of the conical boattail. 2) The square boattail has about the same drag reduction as the conical boattail. 3) The cruciform boattail drag is high, due apparently to low base pressures. 4) The twisted triangular boattail has the best aerodynamic properties for projectiles. It has the lowest drag, good pitching moments, and low Magnus moments for good stability. 5) The new boattails give the projectile long wheel bearing for low balloting while in the gun tube.

## References

[1] Platou, A. S., "An Improved Projectile Boattail," BRL Memorandum Rep. 2395, July 1974, AD 785520, U.S. Army Ballistic Research Labs., Aberdeen Proving Ground, Md. Also AIAA Paper 74-779, Anaheim, Calif., 1974.

[2] Platou, A. S., "Magnus Characteristics of Finned and Nonfinned Projectiles," *AIAA Journal*, Vol. 3, Jan. 1965, pp. 83-90.

[3] Platou, A. S., Colburn, R., and Pedgonay, J. S., "The Design and Dynamic Balancing of Spinning Models and a Testing Technique for Obtaining Magnus Data in Wind Tunnels," BRL Memorandum Rep. 2019, Oct. 1969, AD 699803, U.S. Army Ballistic Research Labs. Aberdeen Proving Ground, Md.

[4] Martin, J. C., "On Magnus Effects Caused by Boundary-Layer Displacement Thickness on Bodies of Revolution at Small Angles of Attack," BRL Rep. 870, June 1955, AD 72055, U.S. Army Ballistic Research Labs., Aberdeen Proving Ground, Md.

[5] Nielsen, G. I. T. and Platou, A. D., "Effect of Boattail Configuration on the Magnus Characteristics of a Projectile Shape at Subsonic and Transonic Mach Numbers," BRL Rep. 1720, June 1974, AD 921823L, U.S. Army Ballistic Research Labs., Aberdeen Proving Ground, Md.

[6] Murphy, C. H., 'Free-Flight Motion of Symmetric Missiles," BRL Rep. 1216, July 1963, AD 442757, U.S. Army Ballistic Research Labs., Aberdeen Proving Ground, Md.

[7] Sylvester, M. A., "Wind-Tunnel Magnus Tests of Cylindrical and Boattail Army-Navy Spinner Projectiles with Smooth Surfaces and 20-MM Equivalent Engraving (Rifling Grooves), BRL Rep. 1758, Feb. 1975, AD B002628L, U.S. Army Ballistic Research Labs., Aberdeen Proving Ground, Md.

[8] Jenke, L. M., "Experimental Magnus Characteristics of Ballistic Projectiles with and without Anti-Magnus Vanes at Mach Numbers 1.5 through 2.5," AEDC-TR-73-162, AFATL-TR-73-188, Dec. 1973, von Karman Gas Dynamics Facility, Arnold Engineering Development Center, Arnold Air Force Station, Tenn.

[9] Jenke, L. M., and Carman, J. C., "Experimental Magnus Characteristics of Ballistic Projectiles with Anti-Magnus Vanes at Mach Numbers 0.7 through 2.5," AEDC-TR-73-126, AFATL-TR-73-150, Dec. 1973, Propulsion Wind-Tunnel Facility, Arnold Engineering Development Center, Arnold Air Force Station, Tenn.